Independence of solitary-cation properties on the atomic neighborhood in $In_{1-x}Ga_xN$ alloys: A novel perspective for material engineering

Francesco Filippone,* Giuseppe Mattioli, and Aldo Amore Bonapasta
Istituto di Struttura della Materia (ISM) del Consiglio Nazionale delle Ricerche, Via Salaria Km 29.5, CP 10, 00016 Monterotondo Stazione, Italy

(Received 21 June 2017; revised manuscript received 13 September 2017; published 29 November 2017)

In InN, a genuine band gap opening observed after hydrogenation has been explained by means of the "solitary cation" model, a multi-H complex in which the central cation, In*, is fully separated from the structure [Pettinari *et al.*, Adv. Funct. Mater. **25**, 5353 (2015)]. Similar effects of H on the host band gap have been observed in In-rich $In_{1-x}Ga_xN$ alloys. Paying attention to these materials, we have theoretically investigated the In* properties against three kinds of disorder, structural, compositional, and configurational, all of them possibly occurring in $In_{1-x}Ga_xN$ alloys. As a first major result we have found that a *same*, general solitary-cation model and mechanism explain the effects of hydrogenation on the electronic properties of both InN and In-rich $In_{1-x}Ga_xN$ alloys. Even more interestingly, in these alloys, both the energetics of the In* solitary cations and their effects on the band gap result to be thoroughly independent of their *atomic neighborhood*, in particular, of the number and spatial distribution of their cation neighbors. Significantly, this implies that band-gap opening effects can be safely predicted in whatever hydrogenated In-rich nitride alloy containing different In companions (e.g., B, Al, or Ga) as well as in InN-containing, unconventional compounds (e.g., ZnO-InN), thus offering novel opportunities for material engineering.

DOI: 10.1103/PhysRevMaterials.1.064606

I. INTRODUCTION

Changing the chemical composition of a semiconductor by replacing some of its native atoms with foreign species, like in the cases of doping or alloying of binary compounds, has always been a common practice to modify and control electronic or optical properties of the material. The same goal has been pursued also in a different way, that is, by introducing an interstitial impurity, like atomic hydrogen, in the semiconductor. This procedure does not change the chemical composition of the material. However, H diffuses easily into the material lattice and forms complexes with native or foreign atoms in the structure, thanks to its small size and high reactivity, thus inducing local chemical changes which modify the material properties [1]. For instance, several studies have faced the H-complexes formation in diluted alloys of N in III-V semiconductors, like $GaAs_yN_{(1-y)}$, where H neutralizes the electronic and structural effects induced by the isoelectronic, foreign species N [2,3]. Moreover, in InN, hydrogen has been shown to be a viable tool to control electronic conductivity [4,5]. While these phenomena are well known and studied, only recently it has been found that H in InN can actually modify the chemistry of the *constituent* atoms of a semiconductor crystal. First, the existence of a novel, multiple, 4-H-complex in $In_{1-x}Ga_xN$ alloys was proposed indeed on the ground of extended x-ray absorbtion fine structure (EXAFS) and x-ray absorption near edge spectroscopy (XANES) measurements, and density functional theory (DFT) calculations [6]. Subsequently, it has been found that in hydrogenated InN the atomic arrangement of that 4-H-complex generates "a solitary cation," that is, an In atom strongly separated from its environment, which actually behaves as a chemically different species, In* [7]. Separation is realized through the concurrent action of the 4 H atoms which form strong N-H bonds with the N nearest neighbors of the In cation. The solitary In*, generated as such, induces remarkable modifications in the electronic properties of the InN nitride. The most important is a genuine band-gap opening, which is experimentally as large as 0.4 eV [7]. Such a blueshift in the band gap is definitely not assignable to a Moss-Burstein effect [8,9]; it has been explained instead in terms of a band anticrossing (BAC) mechanism triggered by solitary cations. Theoretical findings have shown indeed that the H-generated solitary In* induces an isolated electronic state which interacts with the bottom of the conduction band (BCB), pushing it towards higher energies, while the top of the valence band (TVB) remains substantially unchanged [7].

Similar band-gap opening effects have been experimentally observed in hydrogenated $In_{1-x}Ga_xN$ alloys, with x up to 40% [6]. However, measurements in alloys leave several open questions. First, alloying implies three different kinds of disorder around a solitary cation: structural (due to different distributions of In and Ga cations in the material lattice), compositional (induced by different In and Ga contents), and configurational (the one induced by different configurations of In and Ga cations neighboring the solitary cation complex) disorder. Thus, the solitary cation model needs to be validated in $In_{1-x}Ga_xN$ alloys by checking its structural and electronic properties, as well as its energetics, against possible effects of such kinds of disorder. Second, the theoretical moiety of Ref. [7] gives an accurate description of the In* complex in InN as well as of its companion, Ga*, in GaN, while suggesting that the hydrogenation process is effective against band gap opening even in $In_{1-x}Ga_xN$ alloys; since in these alloys the gap opening has been measured only up to Ga concentrations of ≈40%, it was theoretically conjectured this is due to H solubility decreasing as Ga content grows. Even this interpretation of the experimental findings, based on properties of binary compounds, has to be verified by investigating

*francesco.filippone@ism.cnr.it

the properties of H and In* in $In_{1-x}Ga_xN$ alloys. In the present work, we devised, therefore, a series of theoretical simulations, in order to clarify such open points concerning the solitary-cation model in In-rich $In_{1-x}Ga_xN$ alloys.

The achieved results have strengthened the In* model and given a significant, unexpected indication. As a first, major finding, they definitely establish that a *same* model and mechanism, based on the In* (Ga*) complex, can account for the effects of hydrogenation on the band gaps of both InN and $In_{1-x}Ga_xN$ alloys. Moreover, the In* and Ga* complexes present features which are shared by other multi-H complexes forming in InN and GaN, thus giving a more general significance to the solitary-cation model. Finally, as a pleasant surprise, the investigations on disorder effects have given a third and more important indication by showing that the properties of the solitary cations are fully independent on their *atomic environment*. In particular, the formation of In* solitary cations and their effects on the energy gap of In-rich $In_{1-x}Ga_xN$ alloys result to be thoroughly independent of the number and spatial distribution of In or Ga neighbors, that is, a somewhat *local* character of the In* properties dominates the phenomenon of the band-gap opening. Remarkably, this implies that the formation of In* and its effects on the band gap can be predicted in InN-rich nitride alloys as well as in several InN-containing compounds. We will show indeed that, due to such In* local character, the only requirement to be satisfied in InN-containing materials in order to induce a band-gap opening is a prevailing contribution of In *s* states at the material BCB. Such a requirement is expected to be satisfied in several compounds where the InN companion presents a similar work function and a large energy gap, both conditions being favored by the quite large work function (about 5 eV [10]) and the small energy gap (0.78 eV [11]) of InN. Thus, for instance, solitary-cation effects are expected in In-rich nitride alloys where In cations are partially substituted by, e.g., B, Al, or Ga cations [12]. In this case, a third parameter, *alloy stochiometry*, may become available, together with alloy composition and hydrogenation treatments, for a fine tuning of the material band gap and lattice constants. Most important, solitary-cation effects on the band gap are also expected in unconventional materials involving InN, like ZnO-InN alloys [13,14], where InN clusters can be incorporated in the ZnO matrix (work function for ZnO is around 4 eV [15–17]).

The present study has been developed by performing first a deeper investigation of the properties of the In* and Ga* complexes as well as of different multi-H complexes, in InN and GaN binary compounds. The In* and Ga* complexes have been then investigated in $In_{1-x}Ga_xN$ alloys by focusing on the effects of disorder on their energetics and on the mechanism of the band gap opening. See Supplemental Material [18] for further reading about the simulation supercells choice, the approach used here for investigating complex energetics, and the alloys description.

II. THEORETICAL METHODS

We have performed *ab initio* density functional theory (DFT) simulations of the equilibrium atomic structure of both InN and GaN in their most stable hexagonal wurtzite crystal form. We extended the investigations to $In_{1-x}Ga_xN$ alloys with Ga concentrations ranging from 10% to 80%, and compared their electronic and structural properties with the experimental findings. Finally, single- and multihydrogen complexes have been investigated both in InN and GaN as well as in the $In_{1-x}Ga_xN$ alloys with Ga concentrations ranging from 10% to 50%.

TABLE I. Structural data of pure nitride materials. Experimental results are from Ref. [11].

	GaN		InN	
	present	expt.	present	expt.
a (Å)	3.18	3.189	3.57	3.545
c (Å)	5.16	5.185	5.75	5.703
B_0 (GPa)	209	210	146	141
E_g (eV)	3.17	3.50	0.84	0.78

In detail, we used DFT with Hubbard U corrections (DFT + U) [19], as implemented with plane wave basis sets in the QUANTUM-ESPRESSO [20] suite of programs. The plane wave and density cutoffs were 30 and 180 Ry, respectively; the electronic channels, represented by ultrasoft pseudopotentials [21–23], were $2s$ and $2p$ for N; $3d$, $4s$, and $4p$ for Ga; $4d$, $5s$, and $5p$ for In. Hubbard U parameters calibrations as well as equilibrium lattice parameters, bulk moduli, electronic band gaps calculations were conducted using 4-atom wurtzite supercells, with a $8 \times 8 \times 8$ **k**-point Monkhorst-Pack mesh. The Hubbard U correction was applied to the d states of In and Ga and to the $2p$ states of N. The U values were found parametrically for In, Ga, and N in order to reproduce the experimental values of the GaN and InN band gaps and of the position of the Ga and In d shells in the density of states (DOS), as already done in Ref. [24]. The resulting U values are 4.0 eV, 8.0 eV, and 1.0 eV for N($2p$), Ga($3d$), and In($4d$), respectively. The value for N($2p$) is slightly different with respect to what is reported in Ref. [24], in order to describe consistently GaN and InN, together with $In_{1-x}Ga_xN$ mixtures. As the Ga($3d$) [In($4d$)] peaks in the DOS are split, we considered the medium points between the peaks; with the present set of U values, the Ga($3d$) [In($4d$)] levels are located at around 16.5 eV (14.7 eV) from the TVB, in analogy and agreement with literature data [11,25]. Finally, lattice parameters, band gaps, and bulk moduli deviate from experimental values by at most 0.7%, 10%, and 4%, respectively, see Table I.

Unless otherwise stated, all the results we present come from 96-atom orthorhombic supercells obtained from the original 8-atom orthorhombic conventional cell by $2\times3\times2$ replicas along the axes, respectively. Geometry optimizations were performed using a $2\times2\times2$ **k**-point mesh including the Γ point, while electronic dispersions graphs were obtained non-self-consistently starting from potentials calculated on $3\times3\times3$ **k**-point mesh including the Γ point.

A. Multihydrogen complexes in pure InN and GaN

In the present section, we analyze in depth some main features of the solitary cation complex, like its energetics, the role of local strain in its formation, and the close relationship between its structure and the induced BAC effect. Such an

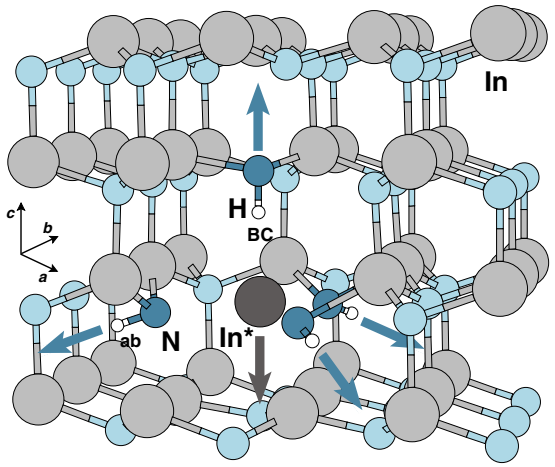

FIG. 1. A schematic view of the In* solitary cation ($3H_{ab} + H_{BC}$ complex) is given. Light gray and light blue circles indicate In and N atoms. Darker gray and blue circles indicate In and N atoms involved in the multi-H complex, white circles indicate H atoms. The arrows indicate the direction of displacements of the complex atoms with respect to the lattice positions. The morphology of the cluster is the same for all the $In_{1-x}Ga_xN$ alloy compositions illustrated in the text, pure GaN included. Note that some atoms have been dropped from the sketch to facilitate the view.

analysis is performed also by comparing the properties of the In* (4-H) complex with those of possible competitors, like complexes containing a smaller number of H atoms, in the cases of the InN and GaN binary compounds. Concepts and results discussed here will be employed in a following section devoted to solitary cations in $In_{1-x}Ga_xN$ alloys.

In InN and GaN, hydrogen typically binds to N atoms, both in antibonding and in bond centered sites. In wurtzite structures, where the c axis is different from a and b axes, the crystal symmetry brings to some anisotropy in the corresponding N-H bonds. Let us introduce the following notation in order to indicate such bonds unambiguously; we use uppercase or lowercase notations when referring to bonds located parallel, or, respectively, out of the c axis. Actually, when one H binds to an N atom parallel to the c axis, in a bond centered position, we indicate it as BC, H_{BC}; analogously, the antibonding location is indicated as AB, H_{AB}. H_{bc} and H_{ab} indicate, respectively, the same bonding locations out of the c axis, see, e.g., Fig. 1. A similar notation will be used also for the multi-H complexes in the following discussion. An isolated H atom is stable at the H_{BC} site. H may also form multicenter bonds when taking the place of a missing N atom in a nitrogen vacancy [5].

The In* configuration, $3H_{ab} + H_{BC}$ in InN, is illustrated in Fig. 1 (the same topology applies to Ga* as well). Here we see that in In*/Ga* complexes, one H binds in H_{BC} location between N and the cation (In or Ga), while three further H atoms locate in H_{ab} positions with respect to the same cation and the three other N neighbors. From a structural point of view, the three N-H_{ab} bonds pull the N atoms away from their respective lattice positions. In this way, room is left around the central cation, thus favoring its displacement induced by the fourth H atom in the BC site.

The inclusion of a single H_{BC} in an In-N bond induces, in its neighborhood, changes of bond distances and bond angles, that is, a local strain. Similarly, the formation of the In* complex induces an even larger local strain. However, the In* geometry arrangement, just illustrated, suggests also the existence of a *cooperative action* of the four H atoms in the complex which may induce a reduction of the local strain with respect to the situation with four separated H_{BC} atoms, in favor of the formation of the In* complex. Such a suggestion is somewhat supported by the fact that the In* configuration is the only one compatible with the results of the mentioned EXAFS and XANES study [6] among the different multi-H configurations considered there. The local strain, therefore, deserves a significant place in the following discussion on the energetics of the In* and multi-H complexes.

We have considered the formation of a multi-H complex, like In*, as a two-step process: First, H atoms enter the sample and form single-H complexes, actually, the stable H_{BC}; second, H atoms migrate in the III-V lattice, where hydrogen has a high mobility [26], and eventually cluster by forming multi-H complexes (see also Supplemental Material [18]). Both steps have been investigated by assuming thermodynamic equilibrium conditions, disregarding, therefore, kinetics. H introduction has been characterized by means of the formation energy of the H_{BC} complex [27]. In general, consider a system Y, for instance InN, where we form a defect involving n hydrogen atoms, nH. The formation energy is

$$E_f(n\text{H-Y}) = E_{tot}(n\text{H-Y}) - E_{tot}(\text{Y}) - n/2E_{tot}(\text{H}_2), \qquad (1)$$

where $E_{tot}(n\text{H-Y})$ is the total energy of the system Y containing an n-H complex, and $E_{tot}(\text{Y})$ is the total energy of the unhydrogenated system Y, both calculated in a consistent computational approach (here, the aforementioned DFT + U); H atoms are taken from an external reservoir, corresponding to the stable molecular state in the gas phase, whose energy is calculated accordingly to the other energies. By means of formation energies E_f from Eq. (1) it is possible to estimate the concentration c of defects in the system with respect to temperature,

$$c = N_{sites} \exp(-E_f/k_B T), \qquad (2)$$

where N_{sites} is the number of possible defect sites in the system, k_B is the Boltzmann constant, T is the temperature [27]. The formation of the H_{BC} complex deserves two further considerations. First, the assumption of thermodynamic equilibrium conditions, though simple and effective, is not perfectly fit to describe the hydrogenation process, where strong nonequilibrium (enormous mass action from H atoms) and high temperature conditions hold, which significantly favor the H loading. Second, the effects of local strain have to be taken into account carefully, because the strain induced by the H_{BC} complex implies an energy cost, thus affecting its formation energy and, in turn, the concentration that the complex may reach in a given material, as estimated through Eq. (2). Such an issue is discussed in detail in the Supplemental Material [18].

The second step leading to the formation of In* concerns the *clustering* of four H_{BC} atoms in the In*, multi-H configuration. This step is characterized by the energy balance between the multi-H configuration and four, isolated H_{BC} atoms in the

host lattice. In this regard, we cannot use formation energies as defined in Eq. (1), which consider the complex formation with respect to a reservoir of H atoms in a gas phase. It is possible, instead, as already done with InN (see Ref. [7] and Supplemental Material [18]), to define a clustering energy of the n-H complex in the system Y, as:

$$E_{\mathrm{cl}}(n\mathrm{H\text{-}Y}) = E_{\mathrm{tot}}(n\mathrm{H\text{-}Y}) - E_{\mathrm{tot}}(n\mathrm{H_{BC}}), \tag{3}$$

where the first term on the right hand side has the same meaning as in Eq. (1), and $\mathrm{E_{tot}}(n\mathrm{H_{BC}})$ is the total energy of the supercell containing a number n of isolated $\mathrm{H_{BC}}$ complexes in their *most stable* configuration. For In* complexes, $n = 4$, and actual simulations of four $\mathrm{H_{BC}}$ complexes in the same supercell have been performed by arranging six random configurations and choosing the lowest energy one as a reference to be compared with the multi-H In*. The same has been performed also for $\mathrm{In_{1-x}Ga_xN}$ alloys, in the following section.

The as defined clustering energy has a clear advantage with respect to the formation energy: having as a reference a reservoir of $\mathrm{H_{BC}}$'s, that is hydrogen atoms already internal to the lattice, the clustering energy includes any possible effects of local strain reduction induced by the complex formation, like those suggested by the cooperative action of four H atoms illustrated in Fig. 1.

We have studied the local strain trend with respect to clusterization by two different paths. First, we have calculated the stress in a simulation supercell containing H atoms in a given atomic arrangement. This gives an indirect estimate, the supercell stress resulting from the effects of the local strain induced by a single- or multi-H complex on the whole system. Second, a more direct indication has been obtained by defining a quantity that should explicate the energy advantages caused by the cooperative action of four clustered H atoms with respect to four isolated ones. We exemplify our approach in the case of the In* complex, but the same arguments apply to other complexes as well. First, we define

$$\Delta E_{\mathrm{str}} = E_{\mathrm{str}}(\mathrm{In}*) - E_{\mathrm{bulk}}, \tag{4}$$

where $E_{\mathrm{str}}(\mathrm{In}^*)$ is the total energy of a supercell with the geometry fixed at the In* complex configuration, stripped of the H atoms, and E_{bulk} is the total energy of the InN supercell. In an ideal process of constructing the complex, first by deforming the structure, and second by adding the H atoms, this quantity estimates the energy needed to displace the lattice atoms from bulk to the In* positions, prior to H insertion. Second, we define

$$\Delta E_{\mathrm{bond}} = E(\mathrm{In}*) - E_{\mathrm{str}}(\mathrm{In}*) - 2E(\mathrm{H_2}), \tag{5}$$

where $\mathrm{E(In^*)}$ and $\mathrm{E(H_2)}$ are the same total energies considered in Eq. (1). This quantity estimates the energy released by the formation of N-H bonds when the H atoms are inserted, in their equilibrium positions, in the strained configuration corresponding to $\mathrm{E_{str}(In^*)}$. Then, we can consider the $\Delta E_{\mathrm{bond}}/\Delta E_{\mathrm{str}}$ ratio, which we shall refer to as bonding-to-strain (BTS) ratio, as a measure of a possible energy benefit that can be achieved when the formation of N-H bonds balances the local strain in a given H complex. Let us note that if the energy advantage per N-H bond is almost constant in different complexes, BTS ratios mainly relate to the energy cost caused by local strain. This seems to occur when the In* complex is compared with four isolated $\mathrm{H_{BC}}$ atoms located in sites corresponding to their minimum energy configuration in InN. In these two complex configurations, we have estimated indeed values of -0.98 eV and -1.02 eV for ΔE_{bond} per H atom and values of 1.4 eV and 1.95 eV for ΔE_{str}, respectively, corresponding to BTS ratios of -0.70 and -0.52. Therefore, the larger, negative value of the In* BTS ratio actually indicates that the atomic arrangement in this complex reduces the cost in energy due to local strain with respect to four isolated $\mathrm{H_{BC}}$ atoms. If we consider the stress variations per H atom, $\Delta\sigma/n_{\mathrm{H}}$, calculated for the In* and the four $\mathrm{H_{BC}}$ complexes, about 11 kbar and 12 kbar, respectively, we have an agreement with the just shown BTS ratios in indicating a strain reduction and therefore a higher stability, for In* with respect to four isolated $\mathrm{H_{BC}}$ atoms. Finally, an $\mathrm{E_{cl}}$ value of -0.76 eV estimated for In* in InN shows an overall energy advantage of clustering four H atoms in the In* configuration [28]. All together, these results show that a cooperative action of the H atoms accompanying the formation of In* induces a local strain reduction by favoring the clustered-H complex.

The above considerations will be taken into account in the following section devoted to In-rich $\mathrm{In_{1-x}Ga_xN}$ alloys, where the formation of In* complexes will be discussed in terms of the $\mathrm{H_{BC}}$ formation energies, of the In* clustering energies, and of the local strain effects. In addition to the overall reduction of local strain that we have just seen, the action of the four H atoms in the In* "solitary" complex leads to a physical separation of the central cation from its neighborhood, as well. Such a separation is closely related to the BAC effect. In fact, the outer electronic s state of the separated cation looses any overlap, and therefore any hybridization, with the electronic states of the rest of the structure, primarily of the N nearest neighbors [7]. Consequently, such an s state confines on the central cation, recovering the spherical symmetry of the free atom (see Ref. [7]). In the electronic energy landscape, such a structural separation, and the ensuing evolution of a solitary cation's s state in an atomiclike s state, induce the displacement in energy of such state from its usual location, on BCB, towards the TVB (see also Fig. 4, top panels). At this point, a band anticrossing (BAC) mechanism may be invoked: The isolated electronic s state pertaining to the solitary cation has indeed a repulsive interaction with the s states of the untouched In atoms, which prevail at the BCB, pushing them towards higher energies, while the TVB remains substantially unchanged.

Describing the structural separation of the central cation from its environment and its effects on the electronic spectrum, an obvious question arises: Are these properties peculiar and unique features of the In* complex? In this regard, we have examined the properties of some multi-H complexes formed by a smaller number of H atoms. For investigating the energetics of such complexes, we have introduced a convenient quantity for a complex involving n H atoms, the association energy, $\mathrm{E_{ass}}\{n\mathrm{H}\}$;

$$E_{\mathrm{ass}}\{n\mathrm{H}\} = E_{\mathrm{tot}}\{[n\mathrm{H}]\} - E_{\mathrm{tot}}\{[(n-1)\mathrm{H}] + [\mathrm{H_{BC}}]\}, \tag{6}$$

where the second term on the right hand side corresponds to the total energy of a supercell containing a complex formed by $(n-1)$ H atoms together with a separated $\mathrm{H_{BC}}$ atom;

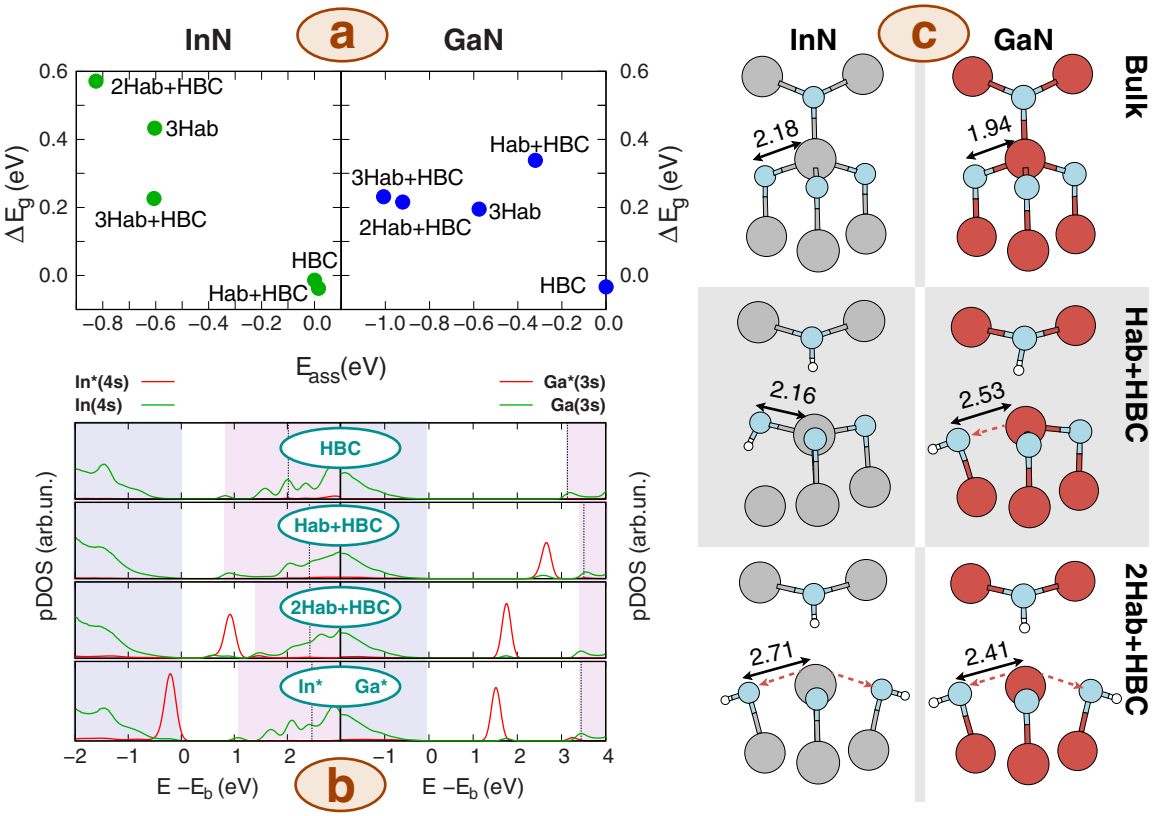

FIG. 2. (a) Band gap shifts induced by the main nH-complexes in InN and GaN, reported as a function of $E_{ass}[n\mathrm{H}]$, Eq. (6); n ranges from 1 to 4 [also in panel (b)]. (b) pDOS of nH complexes. Red lines; projection on the s states of the central cation. Green lines; summed projections on the remaining In (Ga) cations s states. The zero in the energy is located on TVB (E_b in the figure). Shading indicates the energy spans of the VB, light blue, and of the CB, light magenta. Dotted lines represent the Fermi level; for $2H_{ab}+H_{BC}$ in GaN, E_F is slightly out of the energy range. (c) Geometries of representative H complexes in InN and GaN. Gray, red-brown, light-blue, and small white circles represent In, Ga, N, and H atoms, respectively. Relevant distances are shown in Å.

E_{ass} estimates a possible energetic advantage induced by joining an H atom to an $(n-1)$ H complex. Such a quantity, computationally more affordable than the clustering energy, Eq. (3), gives therefore a reliable ground for discussing the complex formation. It may be viewed also in a different way. In fact, if we ideally construct the In* (Ga*) complex adding H atoms one at a time starting from the H_{BC} complex, E_{ass} gives the energy balance of the intermediate steps, each one leading to the formation of a complex involving n H atoms. Should there be an appreciable positive value of E_{ass} for a certain $n<4$, the complex construction would find an obstacle at such n value.

In panel (a) of Fig. 2, we report the band gap shift induced, both for InN and GaN, by a given n-H complex with respect to the corresponding association energy; for H_{BC}, $n=1$ and E_{ass} equal to zero. In panel (b), we show projected densities of states (pDOS) of the same complexes, except the $3H_{ab}$ complex which shows the same properties of the $2H_{ab}+H_{BC}$ one. From panel (a) we see that: (i) all the E_{ass} values are negative, with the only exception of $H_{ab}+H_{BC}$ in InN, which requires a very small energy to form (0.014 eV). Substantially, this means that, starting from the H_{BC}, there is an energetic advantage in adding one H atom to an existing complex, up to the In*/Ga* ($3H_{ab}+H_{BC}$) complex, which is therefore the final product of hydrogenation. (ii) As already known, complexes with just one H atom, H_{BC}, leave the band gap unaffected. (iii) On the contrary, even complexes with less than four H atoms can induce a noticeable band gap shift. More specifically, at least three H atoms must be involved in the complexes to be effective in band gap opening in InN, while two H atoms are sufficient in the case of GaN.

In Fig. 2(b), the pDOS from the s states of the cations other than the complex center, are summed and displayed by green lines, locating on the BCB or deep in the valence band. The red lines, instead, are relative to the s states of the central cation, be it In or Ga, of the complex. In some complexes, such s states localize on the central cations themselves and show an atomiclike character, as it may be drawn with an electron density graph in direct space (not shown here) and separate from the s states of the other cations in the electronic energy diagram, as reported above for the case of In*. More specifically, the pDOS panels show that the onset of a similar In*/Ga*-like state localized on the central cation occurs when $n=2$, i.e., with the $H_{ab}+H_{BC}$ complex in GaN, and when $n=3$, i.e., with the $2H_{ab}+H_{BC}$ complex in InN. There is a close relationship between the electronic state localization and the structural features of the complexes that can be illustrated by means of Fig. 2(c), where the geometries of the complexes relevant to this point are sketched. These geometries show that a strong separation of the central cation occurs in GaN with

the $H_{ab} + H_{BC}$ complex; comparing the Ga-N distances with those in the GaN bulk, the H_{ab} induces a distance growth from 1.94 Å to 2.53 Å between Ga and the N-H_{ab} group together with a distance 2.78 Å for the Ga-(H_{BC})-N pair corresponding to the Ga-N bond broken by the H_{BC}. On the other hand, in InN, the same complex does not induce a strong separation of the central In with respect to its N nearest neighbors. In fact, while the H_{BC} formation increases the In-(H_{BC})-N distance to 3.38 Å, the central In cation remains tightly bound to the three basal N neighbors: The In-N(-H_{ab}) distance shrinks from 2.18 Å in the bulk to 2.16 Å in the complex, the other two In-N distances shrink to 2.13 Å. Moreover, the formation of the N-H_{ab} bond induces an increase of the In-N distance involving a second In atom (2.98 Å), as it might be argued from the sketches in Fig. 2(c). However, also this second In atom keeps the same tight binding pattern with its three basal N neighbors (not shown in the figure) that we have just illustrated. Thus, no In atom is separated from its environment, no solitary atomic *s*-like electronic state arises, and no band gap opening is observed. We note the different reaction to the complex formation in InN with respect to GaN. The Ga cation tends to release the stress by detaching from the two hydrogenated nitrogen atoms, giving rise to the solitary *s*-like electronic state. The central In cation, on the other hand, detaches from a N atom but remains tightly bound to its three basal N neighbors and the stress relief is obtained by strongly weakening a In-N bond pertaining to a second neighbor In atom. The pDOS reported in the panels relative to such two $H_{ab} + H_{BC}$ complexes clearly show the onset of the isolated *s* state in GaN and not in InN. A similar analysis may be performed on the $2H_{ab} + H_{BC}$ complexes; the addition of one H atom to the $H_{ab} + H_{BC}$ complex realizes the cationic detachment in InN, as the In-N distance grows to 2.71 Å. A similar configuration occurs in GaN, and the pDOS panel confirms the onset of the localized state both in InN and GaN. The different features of the $H_{ab} + H_{BC}$ complexes in the two materials may be interpreted in the following way; Ga cations are smaller and less polarizable than In, so a clear detachment from two N neighbors is effective enough to induce a (solitary-cation)-like electronic behavior. On the other hand, in InN a strong separation of the cation from its environment needs one more H atom to take place. Moreover, comparing the results of the (a) and b) panels of Fig. 2, we can state that the occurrence of the atomiclike *s* state always induces the band gap opening, in line with the BAC model. These results build a first part of the answer to the question posed above. They indicate indeed that the mechanism proposed to explain the effects of In* on the band gap can be, to a certain extent, generalized: In InN and GaN, whenever the action of H atoms induces some separation of a cation from its neighbors, an atomiclike *s* state arises, which produces a repulsive interaction with *s* states at the BCB.

The *n*-H complexes, up to $n = 4$, i.e., In*, share a same action on the band gap, as well as an increasing stability with growing *n*; there are two coherent contributions that help in explaining why. The first contribution comes from the strain needed to accommodate the H atoms upon complex formation. As shown above, a rough quantitative measure of local strain effects is represented by the stress variation per H atom, $\Delta\sigma/n_H$, calculated with respect to the pristine material. In InN, $\Delta\sigma/n_H$ values are about 12 kbar for the $3H_{ab}$ and $2H_{ab} + H_{BC}$ complexes, and 16 kbar for the $H_{ab} + H_{BC}$ complex, to be compared with the value of 24 kbar estimated for the isolated H_{BC}. All together, these results are consistent with the aforementioned $\Delta\sigma/n_H$ values for the In* and 4-H_{BC} complexes (11 kbar and, respectively, 12 kbar): The n-H complexes induce an appreciable reduction of the stress with respect to (*n*-1)-H complexes (markedly with respect to H_{BC}), consistent, in turn, with negative E_{ass} values. In other words, cooperative effects of the H atoms, similar to those described in In*, take place also when $n = 3$ and tend to stabilize the complex. Similar considerations can be made for the GaN case, where a negative E_{ass} pertains also to the $H_{ab} + H_{BC}$ complex. The second contribution will be illustrated for the 4-H In* in InN, but the same arguments apply to Ga* as well as to 2- or 3-H complexes in InN, GaN, and $In_{1-x}Ga_xN$ alloys; the occurrence of a (solitary-cation)-like localized *s* state lowers the electronic energy of multi-H complexes against single-H complexes. In fact, the *s* atomiclike state forms right inside the energy gap, displacing from the BCB towards the TVB, while no such occurrence is found for single-H_{BC} complexes. At the same time, we know that hydrogen binds to an N atom as a H^+ ion, loading its electron on the first available electronic state in the nitride band structure. Therefore, if we consider the four H atoms pertaining to the In* complex, four electrons are released to the system; following an *auf bau* ordering, two electrons load on the *s* atomiclike state of the solitary cation, while the further two load on the BCB. On the other hand, when we consider four single-H_{BC} complexes, no atomiclike state displaces from BCB, thus all of the four released electrons load onto the CB, with an energetic disadvantage that can be of the order of the band gap.

In a brief summary, the above results strengthen a general significance of the solitary cation model. They show indeed that in 4-H complexes, like In*, Ga*, as well as in 2- or 3-H complexes: (i) a cooperative action of the hydrogen atoms induces a separation of a cation from its environment as well as a reduction of local strain which favors the complex formation; (ii) a *same* mechanism drives the band gap opening; once a structural separation occurs, an atomiclike *s* state appears which has a repulsive interaction with the BCB *s* states.

Although different multi-H complexes present interesting effects on the band gap, energetics drives towards the formation of the fully hydrogenated In*/Ga* complexes. These results definitely indicate these complexes as the most likely ones in InN and GaN nitrides. We focus therefore on these same two complexes when considering $In_{1-x}Ga_xN$ alloys.

B. Solitary cations in $In_{1-x}Ga_xN$ alloys

In this section, we face the central point of the present paper, that is, the investigation of the effects that different kinds of disorder, structural, compositional, and configurational, in $In_{1-x}Ga_xN$ alloys can produce on the properties of the In*/Ga* complexes. H_{BC} complexes will be also considered for comparison.

Details on our approach for describing binary InN and GaN mixtures, like the $In_{1-x}Ga_xN$ alloys, are given in Sec. II of the Supplemental Material [18], where comparison with literature data is performed [29–32]. Here, we just recall that the trend

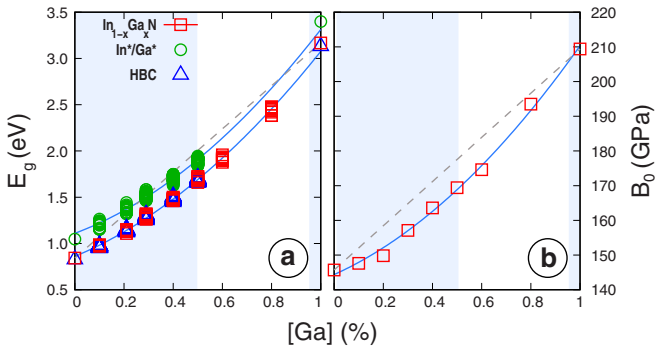

FIG. 3. Trends with respect to Ga content of the alloys. Panel (a): band energy gap. Red squares indicate values from *all* configurations considered for every concentration of pristine alloys. Blue triangles indicate values for all the systems with H_{BC} complex, while green circles represent data for all the systems with solitary cations, either In* or Ga*. A gray dashed line shows the linear behavior of Vegard's law. Light blue lines represent quadratic fits, both for hydrogenated and unhydrogenated alloys. Panel (b): bulk moduli with respect to Ga content. Symbols like in left panel. Shading highlights the region of Ga content where we simulated hydrogenation.

of a given quantity Q_x (for instance the lattice parameter) in binary mixtures, may be expressed with respect to the mixture fraction x in terms of a linear combination of the known quantities Q_A and Q_B, pertaining to the starting materials A and B, plus a corrective quadratic term, whose coefficient b is the bowing parameter;

$$Q_x = xQ_A + (1-x)Q_B + bx(1-x). \tag{7}$$

Present alloys investigations were conducted in two main stages. In the first stage, we simulated pristine $In_{1-x}Ga_xN$ alloys with Ga concentrations x equal to 10%, 21%, 29%, 40%, 50%, 60%, and 79%; for every alloy composition we generated a subset of 12 different random configurations (similarly to what we have already done in previous work [33]) each of which has been optimized in geometry with the same **k**-point sampling of 96-atom binary compounds InN and GaN; further details may be found in Sec. B of the Supplemental Material [18].

The calculated energy gaps corresponding to all of the sampled configurations represent data sets with respect to Ga concentrations and are reported in Fig. 3(a), red squares. Fits to Eq. (7), are shown in Fig. 3(a) with light blue lines. The resulting bowing parameter b is 1.11 eV, to be compared with analogous data reported in literature; 1.7 eV [34], 1.57 eV [30], 1.10 eV [35], 1.3 eV [36,37]. Note that the best agreement between presently calculated bowing parameter and literature data occurs with Refs. [35–37] where beyond-LDA calculations, many with hybrid functionals are performed. Bulk moduli have been also estimated, by varying the simulation volumes; the results are shown in Fig. 3(b), together with a fit to Eq. (7), where b equals 34 GPa.

In the second stage, since we are interested in the In-rich part of alloys [6], we simulated hydrogenation only in the range from $x = 0\%$ (i.e., InN), to $x = 50\%$, together with GaN ($x = 100\%$). For every x in this range, we picked the lowest total energy configuration of the pristine alloy and used it to simulate both a series of 48 H_{BC} structures, as well as a series of 48 In*/Ga* structures, each pointing on every cation available in a 96-atom supercell. In this way, the supercells corresponding to the minimum energy configuration of In* in alloys of *different* compositions take into account the effects of both different In/Ga ratios, that is, compositional disorder, and different distributions of In and Ga cations in the cationic sublattice, that is, structural disorder, on the In* properties. Then, for a given alloy composition, we focus on the configurational disorder by keeping fixed the In and Ga distribution in the cationic sublattice of the simulation supercell and by sampling 48 different In* (Ga*) sites, thus considering all the possible atomic neighborhoods of a solitary cation complex. For supercells containing four H_{BC} atoms, we followed the same procedure we described in Sec. II A, i.e., we chose the lowest energy configuration to give the reference energy to be used in Eq. (3), out of six randomly chosen ones. Finally, we chose the most stable complex configuration to calculate electronic dispersion graphs.

First, we consider the effects of structural and compositional disorder on the electronic properties of In*/Ga* and H_{BC} complexes. The energy gaps estimated in hydrogenated alloys, also reported in Fig. 3(a), show that the H_{BC} complexes do not modify the band gap of the system in which they are simulated. Note, in fact, that the points relative to the H_{BC} complexes (triangles) follow strictly those relative to the pristine alloys (squares). The behavior of H_{BC} complexes with respect to the band gap is, therefore, identical to what we have already seen in discussing pure InN and GaN, see Fig. 2. On the contrary, the blue shift in band gap, already found in InN and GaN, see Fig. 2(a), shows up also in $In_{1-x}Ga_xN$ alloys containing solitary cations, see Fig. 3(a). The points relative to the In*/Ga* complexes lowest in energy (bottom circles for each alloy composition) differ from data relative to unhydrogenated systems, for ΔE_g of $\approx$0.2 eV across the whole compositional range of the alloys ($\Delta E_g = 0.21$ eV for pure InN, while $\Delta E_g = 0.23$ eV for pure GaN). This implies a trend for the energy gap induced by the In*/Ga* complexes which strictly follows that shown by the unhydrogenated alloys. In fact, the bowing parameter b is 1.22 eV for In*/Ga* complexes, close to the 1.11 eV calculated for the unhydrogenated ones. This result is significant, since it shows that the effects of In*/Ga* complexes on the energy gap (i.e., the ΔE_g values) are independent of the alloy's composition and structure. Actually, this result fits pleasantly with our solitary-cation model, mainly based on the repulsion between a *local* electronic state and the BCB.

It is important to note that ΔE_g is also unaffected by configurational disorder: The scattering of the points relative to all of the 48 possible complex configurations (i.e., the set of circles in the figure) for every alloy composition, see Fig. 3(a), is indeed very limited. Thus, on one hand, these results reinforce our model: In fact, the strong, spatial localization of the electronic s state on the ground of the BAC mechanism is in perfect agreement with an independence of ΔE_g's on configurational details, same as on compositional and structural disorders. On the other hand, all together the above results reveal an unexpected and remarkable feature of the In*/Ga* properties: The effects induced by these complexes on the energy gap are fully independent of their atomic neighborhood.

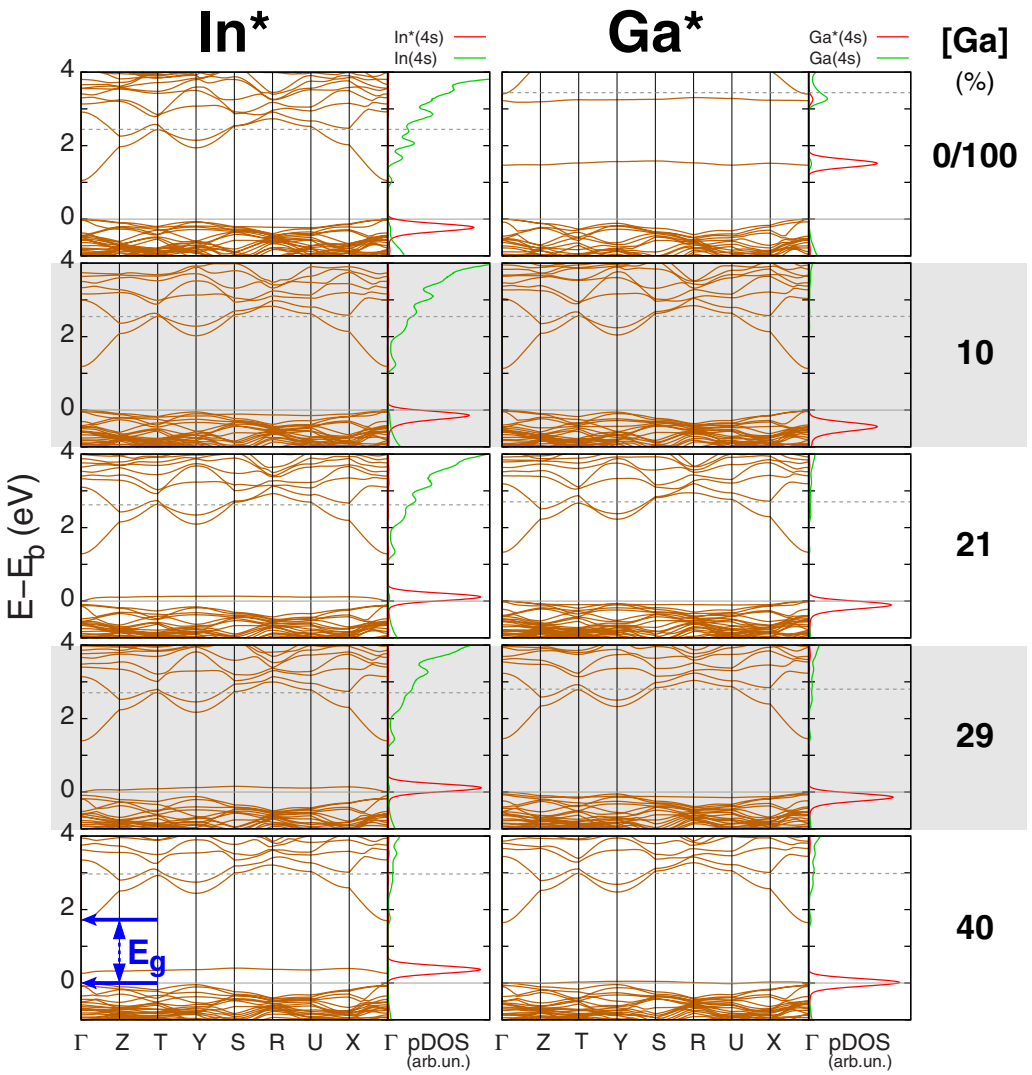

FIG. 4. Dispersion graphs of electronic states for solitary cations at various concentration of Ga. Aside each dispersion graph, the corresponding plot of the density of states projected on some atomic states; red the *s* state of the solitary cations, green the sum of all the other cations' *s* states of the same element. Zero of energy is on TVB (E_b). Dashed gray lines indicate the Fermi level pertaining to each system.

Further details of the In* and Ga* electronic properties are reported in Fig. 4, showing the dispersion graphs of the electronic states in the first Brillouin zone around the Fermi energy for alloy compositions 0% (i.e., InN), 10%, 21%, 29%, 40%, and 100% (i.e., GaN), relative to the most stable In* and Ga* complexes. Together with the dispersion graphs, on the same energy scale, the figure reports the pDOS on the *s* states of both the solitary cations, and the sum of the *s* states of all the cations other than the central, similarly to what was already shown in Fig. 2. The appearance of a localized *s* state belonging to the central cation is evident. In fact, in pristine materials the BCB is composed mainly of *s* states of the In (Ga) cations. When the In* (Ga*) complex forms, the corresponding *s* atomiclike state displaces from BCB and locates in the vicinity of the TVB, as clearly displayed in Fig. 4. These features are shared by all the considered alloys (also 50%, not shown here for the sake of conciseness). Note that contributions from untouched In *s* states contribute mostly to the BCB, since they lie lower in energy with respect to the akin contributions from Ga *s* states. This pictorial representation shows that the operating principle of the BAC mechanism induced by the solitary cations is the same both in $In_{1-x}Ga_xN$ alloys as well as pure InN and GaN. This last result is the ground for the final prediction we reported in the Introduction; a band gap opening may be engineered in InN containing compounds by means of hydrogenation procedures. In fact, nitrides like GaN, or even oxides like ZnO, have a similar work function (≈4.5–5.0 eV) and a definitely larger band gap than InN. Present results regarding InN-GaN mixtures show that the two above conditions are sufficient to achieve a BCB of the final compound mainly composed of In *s* states, and this only requirement assures the onset of a BAC effect.

Let us inspect now if and how alloying disorder affects the energetics of In* or Ga* complexes. Given the description of In*/Ga* complexes formation as a two-step process, we consider separately the disorder effects on the introduction of H in the host material (first step) and on the clustering of

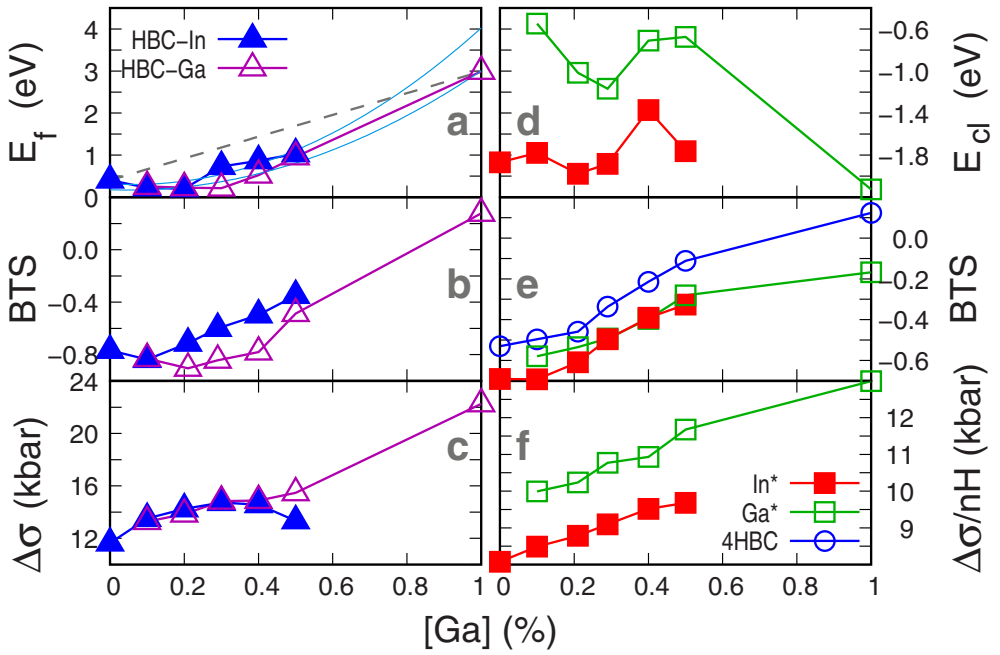

FIG. 5. Left: filled (empty) triangles are relative to H_{BC}-In (H_{BC}-Ga) complexes. Right: filled (empty) squares are relative to In* (Ga*) complexes. Empty circles are relative to 4-H_{BC} configurations lowest in energy. Formation energies for H_{BC} complexes and clustering energies for In*/Ga* complexes are reported in (a) and (d) panels, respectively. BTS ratios are reported in panel (b) for H_{BC} complexes, in panel (e) for In*/Ga* and 4-H_{BC} complexes. Variation of stress ($\Delta\sigma$) per H atom is shown in panels (c) and (f).

the H atoms to form the In* or Ga* complexes (second step). In Fig. 5, the three panels on the left show: (a) formation energies, (b) BTS ratios, and (c) stress $\Delta\sigma$ values for the H_{BC}-In and H_{BC}-Ga complexes with respect to Ga content of the alloys. In the same figure, the three panels on the right show: (d) E_{cl} clustering energies, (e) BTS ratios, and (f) stress variation values, $\Delta\sigma/n_H$, for the In* and Ga* complexes with respect to the Ga content of the alloys. Panel (e) also reports BTS ratios estimated for the minimum energy configurations of four isolated H_{BC} atoms in the simulation supercell (same configurations considered for estimating E_{cl} values). The above quantities are calculated for the minimum energy configuration of each complex.

From panel (a) we see that formation energies of H_{BC} follow a quadratic trend with respect to x, with a minimum for $x = 0.2$. H_{BC}-Ga is the stable complex across all the composition range, except for the smallest Ga concentrations, where H_{BC}-In has a slightly lower formation energy. The stress induced by the H_{BC}-Ga complex increases with the Ga content, see panel (c), while in the case of H_{BC}-In, it reaches a maximum around $x = 0.4$. The BTS ratios calculated for both H_{BC} complexes, see panel (b), show a general agreement with the corresponding formation energies, by increasing with the Ga content. The agreement is very good in the case of H_{BC}-Ga, where the BTS values show a minimum for $x = 0.2$, the same point where the corresponding formation energies show a minimum. These results indicate a close relationship between formation energy and local strain. Stress values give less accurate indications than BTS values by showing, in the case of the stable H_{BC}-Ga, only a rough agreement with the increase of the complex formation energy with the Ga content. These results may be explained as follows. As the Ga content grows, the stiffness of the alloy grows consequently, as witnessed by the growth of the bulk modulus B_0, see Fig. 3. The stiffer the system, the harder the deformation needed to accommodate the H_{BC}. This accounts for an increase of both the BTS values and the H_{BC} formation energy with the Ga content, characterized also by a bowing similar to that shown by B_0 in Fig. 3. Although nonequilibrium conditions drive the loading of H in the $In_{1-x}Ga_xN$ alloys, the above results suggest that the first stage of the In*/Ga* formation process, H introduction in the lattice, suffers for the increase of the alloy stiffness at increasing Ga contents.

Coming now to the effects of compositional and structural disorder on the second stage of the formation process, the clustering of H atoms in the In*/Ga* configuration, the stress values, and the BTS ratios estimated for the In* and Ga* complexes show quite similar trends. Stress values indicate that a larger strain is induced by Ga* with respect to In*, which agrees with the indication given by BTS ratios. These ratios also show that both In* and Ga* reduce the energy cost of local strain with respect to four isolated H_{BC} atoms, thus confirming the energy benefit given by the cooperative action of the H atoms in the solitary-cation configuration even in the case of $In_{1-x}Ga_xN$ alloys. These results fully agree with the clustering energies of panel (d) showing that: (i) In* is always the most stable complex in the whole compositional range and (ii) all of the In* clustering energies are negative, as in InN, thus indicating that a spontaneous formation of the complex is *not affected* by structural and compositional disorder [38].

Finally, Fig. 6 shows the effects of configurational disorder on the energy gap and on the E_{cl} clustering energy of the In* and Ga* complexes, for different alloy compositions.

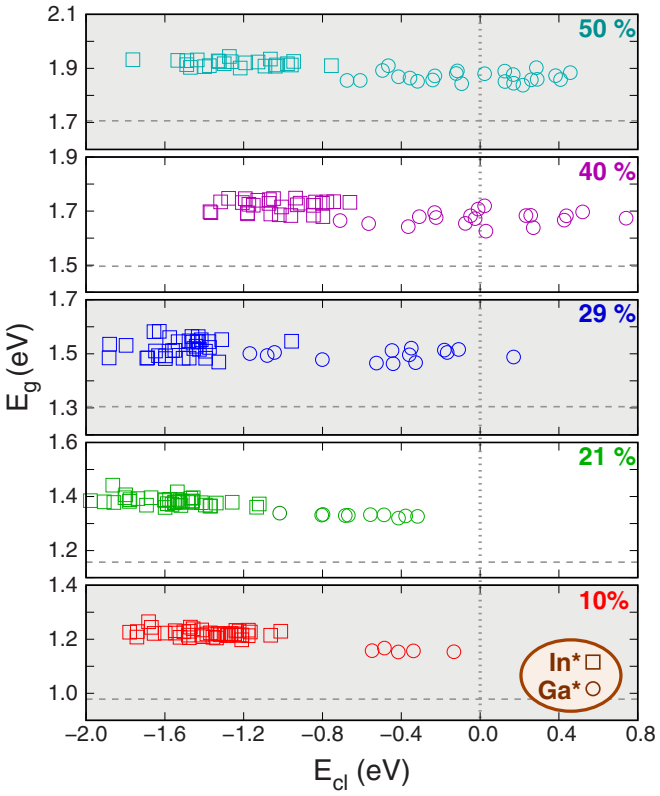

FIG. 6. The band gap of different $In_{1-x}Ga_xN$ alloys containing In* (squares) and Ga* (circles) complexes is reported with respect to the E_{cl} clustering energies of the same complexes. Ga concentration grows from the bottom panel to upper panel. Dashed horizontal lines indicate the band gap relative to the pristine alloys compositions. Zero of energy is highlighted by a vertical dotted line.

As expected, this kind of disorder significantly affects the E_{cl} values. However, in the case of In*, these values are always negative. Therefore, the In* complex spontaneous formation is unaffected by configurational disorder, exactly like structural and compositional disorders, as shown earlier. Figure 6 also shows in some detail how configurational disorder does not affect the amount of the band gap opening.

All together present results: (i) confirm the soundness of the solitary cation model for explaining the H effects on the energy gap of $In_{1-x}Ga_xN$ alloys experimentally observed in the compositional range going from $x = 0\%$ to $x = 40\%$ and (ii) indicate that both the energetics and the electronic effects of the In*/Ga* complexes are fully independent of the three kinds of disorder, that is, of their atomic environment.

Experimental observations state also that the band gap blueshift originated by hydrogenation nullifies when Ga concentration reaches 50%. In the mentioned, previous work [7], we suggested as a possible explanation of this result the different solubility of H in InN and GaN. In detail, we considered that H can form In* and Ga* complexes in the two materials, respectively, and that in both cases these complexes open the host band gap. However, we also estimated a much higher solubility of H in InN with respect to GaN and predicted the absence of H effects on the GaN band gap caused by a too low concentration of H atoms and, therefore, of solitary cations in its lattice. By analogy, we suggested that H and, consequently, In* concentrations in $In_{1-x}Ga_xN$ alloys decrease at increasing Ga content. Such a suggestion, founded on the properties of the binary compounds, has been verified here by using Eq. (2) and the formation energies in 96-atoms supercells [panel (a) of Fig. 5] for direct estimates of the H_{BC} concentrations in the various alloys at $T = 573$ K, the temperature at which hydrogenation takes place experimentally [6,7]. In alloys with x up to 0.3, Eq. (2) estimates H_{BC} concentration around the order of 10^{21} sites/cm^3, which corresponds to In* concentrations high enough to be compatible with experimental observations [39] (see Supplemental Material [18] for a brief discussion about H concentration in presently used simulation supercells). H_{BC} concentration drops of three orders of magnitude when $x = 40\%$ and drops of seven orders of magnitude when $x = 50\%$. As stated above, hydrogenation procedures are performed at nonequilibrium conditions. Notwithstanding, present results agree with a dramatic decrease of the In* concentration, induced by a lower efficiency of the hydrogenation procedure when the Ga content in the alloy reaches the value $x = 50\%$, which can account for the experimental findings and agrees with the above considerations on the increase of the stiffness of the alloys at increasing Ga content.

III. CONCLUSIONS

A solitary-cation model was proposed in a previous study to explain the experimental observation of the band gap opening in InN upon hydrogenation. This model founds on three main features: (i) the introduction of H in the structure promotes the separation of an In cation from its own neighbourhood through the formation of a multi-H complex, also referred to as In*, favored by a cooperative action of four H atoms; (ii) such a separation generates an atomiclike, localized s state on the In cation, which also separates from its companion states in the BCB by moving close to the TVB; (iii) this s state interacts with the s BCB states of the untouched In cations according to a band anticrossing model, thus repelling the BCB towards higher energies. Experimentally, similar band gap opening effects were observed also in $In_{1-x}Ga_xN$ alloys upon hydrogenation up to a 40% of Ga content. The effect vanishes for a 50% of Ga content. We have here validated the solitary-cation model in these alloys, investigating the electronic properties and the energetics of In* and Ga* complexes against three different kinds of disorder, structural, compositional, and configurational, which may occur in $In_{1-x}Ga_xN$ alloys. Regarding the energetics, we have considered the formation of the multi-H In*/Ga* complexes as a two-step process: In a first step, H is included in the alloy lattice as a H_{BC} complex; in a second step, the clustering of four H_{BC} atoms leads to the formation of the In*/Ga* complexes. Thus, disorder effects have been considered separately for each step of the process.

Preliminarily, we have analyzed in depth the main features of In* and Ga* by comparing their properties with those of possible competitors, i.e., multi-H complexes involving less than four H atoms, in the binary InN and GaN compounds. The results of such an analysis show that In*, Ga*, and other multi-H complexes share similar (solitary-cation)-like

structural features as well as a same mechanism which can induce a band gap opening, thus giving a more general significance to the proposed model. They also show that In* is the most stable complex in InN.

Then, in the case of $In_{1-x}Ga_xN$ alloys, the investigation of the In*/Ga* complexes has given three main results. First, with x up to a 50% of Ga content, none of the three considered kinds of disorder modifies the effects of solitary cations on the host electronic properties as well as the features of the band anticrossing mechanism. That is, once formed, In* and Ga* complexes induce a band gap opening as they do in the corresponding binary compounds. Single hydrogen complexes have no effect on the alloy band gap, as already found in the case of InN and GaN.

Second, the formation of multi-H In*/Ga* complexes, that is, the clustering of four single-H, H_{BC}, complexes is favored by the cooperative action of four H atoms in these complexes that: (i) reduces the overall local strain induced, separately, by four H_{BC} complexes in the host lattice and (ii) induces the onset of an s-like state localized on the central cation and in the energy gap, which is filled by the electrons released by the H atoms, giving an advantage in electronic energy. Moreover, the clustering process leading to the formation of In* is *always* favored in energy, that is, isolated H atoms spontaneously cluster to form this complex without being affected by disorder effects. These results confirm therefore the presence of In* complexes in $In_{1-x}Ga_xN$ alloys, previously suggested to explain EXAFS and XANES results, and account for the observed band gap opening in the same alloys.

Third, results regarding the effects of alloy composition on the first step of the process suggest that the H concentration in $In_{1-x}Ga_xN$ alloys dramatically decreases when the Ga content reaches the value $x = 50\%$. This implies a corresponding, significant decrease of solitary cations concentration for that Ga content, which fully accounts for the experimental findings.

Overall, two major results have been achieved in the present study. First, it is shown that a *same*, general model can explain the effects of hydrogenation on the electronic properties of InN and In-rich $In_{1-x}Ga_xN$ alloys. A most important and unexpected finding is that the formation of the In* solitary cations and their effects on the host band gap result to be *fully independent* of the complex atomic environment, that is, of the number and spatial distribution of the In and Ga cations around the complex. This indicates that the *local* character dominates the In* properties, in particular, its energetics and its effects on the band gap. In turn, this permits us to formulate a significant prediction: A band gap opening can be realized in whatever hydrogenated InN-containing compound where In s states prevail at the BCB. In fact, present results indicate that in such a material, the clustering of H atoms to form In* solitary cations in an InN region is favored in energy and, thanks to the local character of its properties, the formation of In* generates a spatially localized, atomiclike s orbital which pushes up the In s states forming the BCB, independently of the complex neighborhood. The above requirement regarding the contribution of In s states to the BCB is expected to be satisfied in several compounds, thanks to the quite large work function and the small energy gap of InN. Thus, for instance, the effects of solitary cations are expected to occur in InN-rich alloys where In cations are substituted by B, Al, or Ga cations in whatever relative ratio. In this case, a third parameter, *alloy stoichiometry*, becomes also available, together with alloy composition and hydrogenation treatments, for a fine tuning of the band gap, as well as of the lattice parameters. Remarkably, solitary-cation effects on the band gap are also expected to occur in unconventional materials containing InN, like in the case of ZnO-InN alloys, where InN clusters are incorporated in the ZnO matrix [13,14,17], thus paving novel ways for material engineering.

ACKNOWLEDGMENT

The authors acknowledge Prof. M. Capizzi for the useful observations on the paper.

[1] C. G. Van de Walle and B. Tuttle, IEEE Trans. Electron Devices **47**, 1779 (2000).
[2] A. A. Bonapasta, F. Filippone, and G. Mattioli, Phys. Rev. Lett. **98**, 206403 (2007).
[3] L. Amidani, G. Ciatto, F. Boscherini, F. Filippone, G. Mattioli, P. Alippi, F. Bondino, A. Polimeni, M. Capizzi, and A. A. Bonapasta, Phys. Rev. B **89**, 085301 (2014).
[4] A. Janotti, J. L. Lyons, and C. G. Van de Walle, Phys. Status Solidi A **209**, 65 (2012).
[5] C. G. Van de Walle, J. L. Lyons, and A. Janotti, Phys. Status Solidi A **207**, 1024 (2010).
[6] M. De Luca, G. Pettinari, G. Ciatto, L. Amidani, F. Filippone, A. Polimeni, E. Fonda, F. Boscherini, A. A. Bonapasta, D. Giubertoni, A. Knübel, V. Lebedev, and M. Capizzi, Phys. Rev. B **86**, 201202 (2012).
[7] G. Pettinari, F. Filippone, A. Polimeni, G. Mattioli, A. Patanè, V. Lebedev, M. Capizzi, and A. A. Bonapasta, Adv. Funct. Mater. **25**, 5353 (2015).
[8] E. Burstein, Phys. Rev. **93**, 632 (1954).
[9] T. S. Moss, Proc. Phys. Soc. Sect. B **67**, 775 (1954).
[10] W. Liu, Y. Luo, Y. Sang, J. Bian, Y. Zhao, Y. Liu, and F. Qin, Mater. Lett. **95**, 135 (2013).
[11] I. Vurgaftman and J. R. Meyer, J. Appl. Phys. **94**, 3675 (2003).
[12] The values of the BN, AlN, and GaN work functions are in the range 4.5–5.0 eV, quite close to that of InN, about 5 eV. the corresponding energy gaps, 6.4 eV, 6.2 eV, and 3.4 eV, in the order, are much larger than that of InN, 0.78 eV. These data support the qualitative considerations reported in the text.
[13] C.-H. Shih, I. Lo, W.-Y. Pang, and C.-H. Hiseh, J. Phys. Chem. Solids **71**, 1664 (2010).
[14] M. Dou and C. Persson, Crystal Growth and Design **14**, 4937 (2014).
[15] A. Kumar, T. S. Herng, K. Zeng, and J. Ding, ACS Appl. Mater. Interfaces **4**, 5276 (2012).
[16] A. Sharma, M. Untch, J. S. Quinton, R. Berger, G. Andersson, and D. A. Lewis, Appl. Surf. Sci. **363**, 516 (2016).

[17] Similarly to the case of In-rich nitride alloys discussed above, a ZnO work function (about 4 eV) close to that of InN and a quite larger ZnO band gap (about 3 eV against 0.78 eV) support the occurrence of a BCB mainly contributed by In *s* states in ZnO-InN compounds.

[18] See Supplemental Material at http://link.aps.org/supplemental/10.1103/PhysRevMaterials.1.064606 for a detailed discussion around the effects of supercells dimensions and H concentration on the defect formation energies, as well as around the presently used description of InGaN alloys.

[19] B. Himmetoglu, A. Floris, S. de Gironcoli, and M. Cococcioni, Int. J. Quantum Chem. **114**, 14 (2014).

[20] P. Giannozzi, S. Baroni, N. Bonini, M. Calandra, R. Car, C. Cavazzoni, D. Ceresoli, G. L. Chiarotti, M. Cococcioni, I. Dabo, A. Dal Corso, S. de Gironcoli, S. Fabris, G. Fratesi, R. Gebauer, U. Gerstmann, C. Gougoussis, A. Kokalj, M. Lazzeri, L. Martin-Samos, N. Marzari, F. Mauri, R. Mazzarello, S. Paolini, A. Pasquarello, L. Paulatto, C. Sbraccia, S. Scandolo, G. Sclauzero, A. P. Seitsonen, A. Smogunov, P. Umari, and R. M. Wentzcovitch, J. Phys.: Condens. Matter **21**, 395502 (2009).

[21] D. Vanderbilt, Phys. Rev. B **41**, 7892 (1990).

[22] A. M. Rappe, K. M. Rabe, E. Kaxiras, and J. D. Joannopoulos, Phys. Rev. B **41**, 1227 (1990).

[23] A. M. Rappe, K. M. Rabe, E. Kaxiras, and J. D. Joannopoulos, Phys. Rev. B **44**, 13175 (1991).

[24] F. Filippone, G. Mattioli, P. Alippi, and A. A. Bonapasta, Phys. Rev. Lett. **107**, 196401 (2011).

[25] L. C. de Carvalho, J. Furthmüller, and F. Bechstedt, Appl. Phys. Lett. **102**, 172105 (2013).

[26] A. Janotti and C. G. Van de Walle, Appl. Phys. Lett. **92**, 032104 (2008).

[27] C. G. Van de Walle and J. Neugebauer, J. Appl. Phys. **95**, 3851 (2004).

[28] The E_{cl} value of -0.76 ev, calculated in the 96-atom supercell, has been checked in the 360-atom supercell, where an E_{cl} value of -1.66 ev has been achieved.

[29] I. Gorczyca, T. Suski, N. E. Christensen, and A. Svane, Phys. Rev. B **83**, 153301 (2011).

[30] L. C. de Carvalho, A. Schleife, J. Furthmüller, and F. Bechstedt, Phys. Rev. B **85**, 115121 (2012).

[31] M. G. Ganchenkova, V. A. Borodin, K. Laaksonen, and R. M. Nieminen, Phys. Rev. B **77**, 075207 (2008).

[32] J. A. Chan, J. Z. Liu, and A. Zunger, Phys. Rev. B **82**, 045112 (2010).

[33] L. Amidani, F. Filippone, A. A. Bonapasta, G. Ciatto, V. Lebedev, A. Knübel, and F. Boscherini, Phys. Rev. B **86**, 155211 (2012).

[34] I. Gorczyca, S. P. Łepkowski, T. Suski, N. E. Christensen, and A. Svane, Phys. Rev. B **80**, 075202 (2009).

[35] P. G. Moses, M. Miao, Q. Yan, and C. G. Van de Walle, J. Chem. Phys. **134**, 084703 (2011).

[36] R. R. Pelá, C. Caetano, M. Marques, L. G. Ferreira, J. Furthmüller, and L. K. Teles, Appl. Phys. Lett. **98**, 151907 (2011).

[37] R. R. Pela, M. Marques, and L. K. Teles, J. Phys.: Condens. Matter **27**, 505502 (2015).

[38] Clustering energy has been confirmed to be negative also in test calculations on a 360-atom supercell with Ga content of 50%, with ordered occupation of cationic sites.

[39] D. Dagnelund, W. Chen, and I. Buyanova, in *Hydrogenated Dilute Nitride Semiconductors*, edited by G. Ciatto (Pan, Stanford, 2015), pp. 75–98.